Case Studies in Chemical and Environmental Engineering 11 (2025) 101084

Contents lists available at ScienceDirect

Case Studies in Chemical and Environmental Engineering

journal homepage: www.sciencedirect.com/journal/case-studies-in-chemical-and-environmental-engineering

Case Report

Effect of atomic ratio of ions on the particle diffusion and permeability of carbon nanotubes in reverse electrodialysis process using molecular dynamics simulation

Ali B.M. Ali [a], Karwan Hussein Qader [b], Murtadha M. Al-Zahiwat [c], Narinderjit Singh Sawaran Singh [d], Soheil Salahshour [e,f,g], S. Mohammad Sajadi [h], Ali Mokhtarian [i,*]

[a] Air Conditioning Engineering Department, College of Engineering, University of Warith Al-Anbiyaa, Karbala, Iraq
[b] Department of Computer Science, Cihan University-Erbil, Kurdistan Region, Iraq
[c] Department of Chemical engineering, College of Engineering, University of Misan, Amarah, Iraq
[d] Faculty of Data Science and Information Technology, INTI International University, Persiaran Perdana BBN, Putra Nilai, Nilai, 71800, Malaysia
[e] Faculty of Engineering and Natural Sciences, Istanbul Okan University, Istanbul, Turkey
[f] Faculty of Engineering and Natural Sciences, Bahcesehir University, Istanbul, Turkey
[g] Faculty of Science and Letters, Piri Reis University, Tuzla, Istanbul, Turkey
[h] Department of Chemistry, Payam e Noor University, Saqqez Branch, Kurdistan, Saqqez, Iran
[i] Department of Mechanical Engineering, Khomeinishahr branch, Islamic Azad University, Khomeinishahr, Iran

ARTICLE INFO

Keywords:
Electrodialysis
Reverse electrodialysis
Channel geometry
Carbon nanotube
Molecular dynamics simulation
Atomic ratio

ABSTRACT

This study employed molecular dynamics simulations to investigate water transport through a carbon nanotube under an electric current, focusing on how varying ion atomic ratios influence key system parameters. These parameters include electric current intensity, fluid current intensity, maximum density, hydrogen bond count, and interaction energy as ion concentration changed. The research aimed to examine the effects of these changes on ion mobility, water permeability, and ion–carbon nanotube interactions. The study is conducted in two phases: equilibration, followed by the analysis of atomic transformations and the creation of various atomic ratios in samples. In the first phase, the kinetic energy of the atomic sample converges to 0.162 eV, and the potential energy reaches to 2.048 eV after 10 ns, indicating limited structural mobility and attractive forces among atoms. After equilibration, we achieved the atomic transformation process and created different atomic ratios. The results indicate that increasing ion ratios in the fluid led to a rise in electric current intensity, from 5.31 to 5.52 e/ns. Higher ion concentrations resulted in a greater density of charge carriers, enhancing ionic mobility and ion transport through the carbon nanotube. Moreover, higher ionic concentrations not only reduced the maximum density from 4.83 to 4.65 atoms/nm^3 but also increases the number of broken hydrogen bonds, which could impact water transport and flow dynamics. Finally, according to the findings, there are 133 broken hydrogen bonds instead of 116, and the strength of the nanofluid flow, as well as the electric current, both increased when the ionic percentage of atoms rose to 5 %.

1. Introduction

The global rise in water demand is driven by population growth and industrial activities. This growing demand directly correlates with a rapid decline in water availability and poses significant public health risks from waterborne diseases [1–3]. Addressing these issues requires innovative water purification technologies, particularly for removing dissolved salts [4]. These technologies are categorized into membrane-based and heat-based methods, with membranes playing a vital role in water and wastewater treatment [5,6]. Membrane technologies fall into two main types: pressure-driven and electric-potential-driven systems [7]. Electric-potential methods rely on ion exchange resins, which include cation exchange resins for positive ions and anion exchange resins for negative ions [8,9]. Key technologies in this category ED, Electro-deionization, and RED excel in desalination.

* Corresponding author.
E-mail address: ali.mokhtarian@iaukhsh.ac.ir (A. Mokhtarian).

https://doi.org/10.1016/j.cscee.2024.101084
Received 4 October 2024; Received in revised form 21 December 2024; Accepted 24 December 2024
Available online 25 December 2024

Nomenclature

CNTs	Carbon Nanotubes
RED	Reverse Electrodialysis
NF	Nano Fluid
MD	Molecular Dynamics
BNNTs	boron nitride nanotubes
T	Temperature

RED, in particular, efficiently processes highly saline water without requiring chemical agents, thanks to its ability to reverse electric charges [10]. Innovative advancements include the use of CNTs in membrane systems. These nanoscale structures, known for their exceptional strength, conductivity, and specific surface area, enhance ion transport by modulating factors like ion concentration, surface charge, and pore size [11,12]. CNTs are especially critical for optimizing energy conversion in RED systems. However, challenges such as irregular ion pathways at certain voltages persist [13]. Beyond water purification, CNTs find applications in diverse fields, including energy storage, nanoelectronics, and catalysis, due to their lightweight, cost-effective, and versatile properties [14]. Based on prior studies, scientists employed electrolysis, reverse electrolysis, and reverse osmosis. They also used computer simulations, such as MD, to separate ions from nanofluids (NFs) in various configurations. Researchers investigated the ways to use reverse ED devices to generate sustainable and clean power. Their focus is on the changes in salinity between river and sea water. We can observe the progress of this process by examining the conducted research.

Fatahi et al. [15] investigated the separation and selective removal of toxic heavy metal ions from water by magnetic ion-blocking nanopolymers. The results show that using ion-blocking polymer techniques on the surface of magnetic nanoparticles increases their selectivity, enhancing the removal of metal ions. Lehrasbi et al. [16] studied how to separate ions and purify water using a force created by an electric field on a porous graphene membrane. The findings proved that the distance among the ions was greatly enhanced when the strength of the electric field increased. Khataee et al. [17] studied how to remove nitrate ions from water using tiny tubes made of silicon carbide. The results indicate that nitrate ions can be effectively eliminated from water using SiC-NTs. Othman et al. [18] conducted research focusing on RED, developing an integrated system capable of simultaneous power generation and water treatment. This study indicated that using an integrated RED system is an effective method for energy collection while also mitigating environmental damage from liquid waste disposal. Hong et al. [19] reviewed all the studies undertaken in the field of membrane creation. In addition, they investigated the performance of the existing membranes in ED and RED processes. The key factors examined in these membranes included their ion transfer ability, strength, response to heat and chemicals, and the specific ions allowed to pass through. Li et al. [20] found a way to save energy and handle salt water using RED and reverse osmosis. Moreover, they found a method for regulating the amount of salt water discharged into the environment, which helped safeguard water and land while enhancing conservation and retrieval efforts. They used a method called RED to do this. Yip et al. [21] investigated the comparison of energy efficiency and power density in delayed pressure osmosis and RED. Panahi et al. [22] used MD simulations to study the effect of single-walled-CNTs chirality on the electrokinetic transport of water and ions. The results indicate that ion transport was substantially affected by the chirality of SWCNTs, with zigzag NTs exhibiting higher ion permeability than armchair NTs. Furthermore, this investigation provided valuable insights into the importance of SWCNT chirality in regulating ion permeability and selectivity, a factor essential for applications, such as RED. Shi et al. [23] explored using a new type of NTs, BNNTs, for ion separation and water purification through MD simulations. The results indicate that BNNTs had superior ion selectivity and permeability, surpassing conventional CNTs in ion separation and water desalination. Furthermore, the research highlighted the potential of BNNTs as a highly promising membrane material for RED and various other water treatment applications. Naghdian et al. [24] investigated using borophene, a two-dimensional material, as a membrane for ion separation in the ED desalination process using non-equilibrium MD simulations. The results indicate that borophene membranes possessed extraordinary ion selectivity and permeability, enabling the efficient separation of ions and the purification of water. Additionally, this research provided a comprehensive understanding of how to design and optimize borophene-based membranes for advanced water treatment technologies, such as RED. Hasanzadeh et al. [25] studied the use of a graphene oxide membrane for separating chromium ions from water through MD. The membrane was functionalized with –F, –H, and –OH groups to enhance performance. Additionally, external voltages were applied to improve separation efficiency. Various analyses showed that the modified GO membrane effectively separated chromium ions when proper voltage was applied, making it a promising option for removing heavy metals from water. Li et al. [26] explored the role of channel roughness in improving water desalination using RED with CNTs through MD simulations. Their findings revealed that rough surfaces intensified fluid-wall interactions, which limited particle movement due to stronger forces. The armchair-edged CNT configuration delivered the best electric current output. Additionally, roughness increased the number of broken hydrogen bonds in the water from 116 to 128. The study underscored how CNT surface properties shaped the efficiency of the desalination process. Jasim et al. [27] investigated the effect of an external force (EF) on particle dispersion, channel morphology, and permeability through CNTs in RED systems using MD simulations. The results show that as EF increased from 0.0001 to 0.0005 eV/Å, the electric current rose from 5.31 e/ns to 5.62 e/ns. Meanwhile, fluid flow intensity increased from 211.31 atoms/ns to 263.01 atoms/ns. Additionally, the particle density decreased from 4.83 atom/nm^3 to 4.66 atom/nm^3, while the number of broken hydrogen bonds increased from 116 to 166.

The growing global demand for water, driven by population growth and industrialization, coupled with the rapid depletion of water resources, underscores the urgent need for advanced water purification technologies. Among these technologies, RED systems gained prominence for their potential to efficiently generate renewable energy from salinity gradients. These systems rely heavily on ion transport across specialized membranes, with single-walled CNT-based membranes emerging as promising candidates due to their exceptional structural and functional properties. However, optimizing their performance necessitates a deeper understanding of how specific factors influence ion transport and permeability. This study addressed a critical gap in the literature by focusing on the atomic ratio of ions as a key parameter affecting ion dispersion and transport in SWCNT membranes. Unlike prior research that explored broader aspects of membrane technologies, this work employed MD modeling and provides an atomistic analysis of how the atomic ratio influenced electric current intensity, ion density, hydrogen bonding, and interaction energy. These insights were pivotal for enhancing the design and performance of CNT-based RED systems. Beyond its scientific contributions, the study had significant industrial applications. By elucidating the mechanisms underlying ion diffusion and membrane permeability, it offered a framework for optimizing SWCNT-based RED systems, enhancing their application in water purification and renewable energy production. This innovative focus the atomic ratio of ions as a controlling factor distinguished this research and provided practical strategies for improving the efficiency and sustainability of next-generation desalination and energy systems.

2. Simulation details

The focus of this study was to analyze the effect of CNTs on water movement in a nanochannel using LAMMPS software. The nanochannel in the simulation box was 60 Å long in y and z directions and 260 Å wide in the x-direction. Each compartment was 60 Å in size and contained 10,000 water molecules arranged in a cubic formation. Concurrently, CNTs were positioned in the center of a 105-long nanochannel. VMD software was used to model silicon plates, water molecules, and CNTs. The pristine sample modeled consisted of 38,916 atoms, with ion ratios varying from 1 % to 5 % compared to the pristine sample. Following that, these were combined using PACKMOL software, and water molecules were simulated using the TIP3P model. Silicon membranes were present on both ends of CNTs (see Fig. 1). In three dimensions, periodic boundary conditions were in effect. The time step for the simulation was 0.01 fs, and the simulation time was set to 20 ns, with an initial T = 300 K. Nose-Hoover thermostat was used to maintain a constant T inside the simulated system. The atoms interacted in the simulated systems once the atomic structures were created. The silicon plates were firmly fixed in place and could not be moved. van der Waals interactions were the primary means by which silicon interacted with other atoms in the system. Finding the atoms' positions and the forces exerted on them was the first stage in the process, followed by adjusting the initial values to see if the models reached equilibrium. This necessitated the use of NVT. Additionally, an external electric field with an intensity of 0.01 V/Å and an external force of 0.0001 eV/Å were uniformly applied to the fluid sample. This simulation setup caused the water molecules to be displaced inside the designed system. All of our MD simulation settings are listed in Table 1.

Table 1
Simulation settings in current computational research.

Computational Parameter	Parameter Ratio/Setting
MD Box Length	$60 \times 60 \times 260$ Å^3
Number of Atoms in Pristine Sample	38916
Boundary Condition	Periodic (in all directions)
Thermostat Type	Nose-Hoover
Barostat Type	Berendsen
MD Ensembles	NVT and NVE
Time Step	0.01 fs
Simulation Time	20 ns

3. The equilibration process

To ensure thermodynamic equilibrium in the system, key physical variables, such as potential and kinetic energy were closely monitored throughout the simulation process numerically, with the kinetic energy reaching a value of 0.162 eV after 10 ns. As the particles moved and interacted, they experienced attractive forces from neighboring particles, which gradually slowed down their mobility. Eventually, the motion of atoms became constrained, and the system reached a point where the atoms could no longer move freely, indicating that the structure was stabilizing. The system's stability was maintained due to the balance between the increasing kinetic energy and the attractive forces acting among the atoms. These forces helped prevent the structure from fragmenting or becoming unstable, maintaining a cohesive arrangement despite increasing energy. As a result, the atomic structure reached thermodynamic equilibrium, ensuring stability under the simulation conditions. On the other hand, the atomic system evolved over time, with potential energy computed based on atomic interactions. The simulation results revealed that the potential energy of the system stabilized at 2.048 eV, reflecting the balance of forces acting among atoms, including electrostatic, van der Waals, and other interactions. As the simulation progressed, atoms adjusted their positions, moving toward an equilibrium state that minimized the system's total energy. At 2.048 eV, the atoms reached a stable configuration where attractive and repulsive forces were balanced. Initially, atoms were placed randomly or in predefined arrangements. Over time, atomic interactions drove the system to a state of minimal energy, with the atoms finding an equilibrium position. Once the potential energy stabilized at 2.048 eV, the atoms were in their most energetically favorable state; any deviation from this configuration increased the potential energy, disrupting the stability of the system.

4. Results and discussion

Fig. 2 presents the atomic structure of the target fluid at the final stage of MD simulations, showing atomic ions at concentrations of a) 1 %, b) 2 %, c) 3 %, d) 4 %, and e) 5 %. The main objective of the simulation was to analyze how various ion concentrations affected the stability of the NF system. At higher atomic ratios, ions tended to aggregate, either through interactions with each other or by sticking to the channel walls. This aggregation disrupted the uniform distribution of ions, leading to instability and affecting overall fluid behavior. The graphical outputs in Fig. 2 illustrate the stability of NF flow at different ion concentrations. At lower ion concentrations (1 % and 2 %), NF remained stable, with minimal ion aggregation and a more consistent flow. However, as the ion concentration increased to 3 %, 4 %, and 5 %, the aggregation of ions became more pronounced, which disrupted fluid dynamics and increased instability. These changes in ion interactions with the fluid and channel walls led to higher resistance and less efficient flow. The observed increase in current intensity for Ion Ratio-1% compared to Ion Ratios-2% and 3 % can be explained by the behavior of ions within the nanofluid. At Ion Ratio-1%, the low concentration of ions allowed for greater mobility and minimal aggregation. With fewer ions in the system, they experienced less resistance, facilitating smoother transport and leading to higher current intensity. In contrast, as the Ion

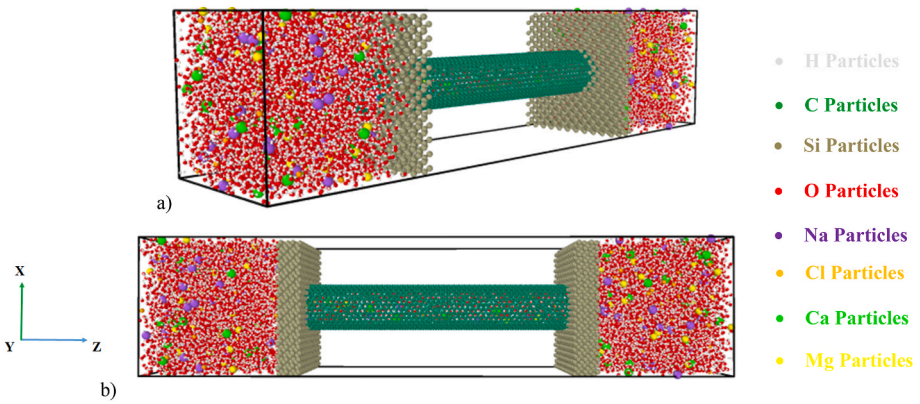

Fig. 1. A view of the atomic arrangement of simulated structure from a)perspective and b)side view.

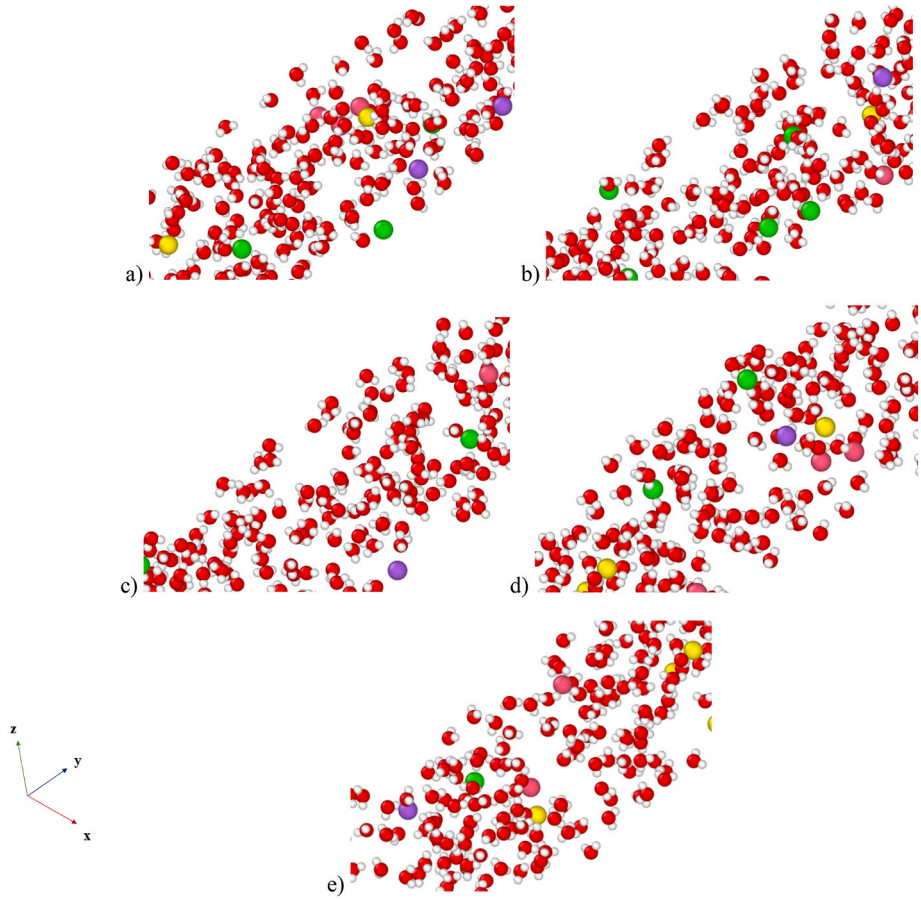

Fig. 2. The atomic structure of the target NF in the last step of MD simulations in the presence of a) 1 %, b) 2 %, c) 3 %, d) 4 %, and e) 5 % of atomic ions.

Ratio increased to 2 % and 3 %, the higher concentration led to more ion-ion interactions and adhesion to the channel walls. This clustering increases resistance and reduces ion mobility, causing a decrease in current intensity. The interaction energy applied to ions in these samples supported this explanation. Numerically, the average interaction energy of each ion in the presence of 1 % was −0.63 kcal/mol. This value increased to −0.71 kcal/mol for 2 % ions and −0.76 kcal/mol for 3 % ions. In conclusion, the findings emphasized the significant role of ion concentration in the stability of NFs.

The net interaction force between the wall and NF particles was calculated to further analyze the effects of the ion ratio on the evolution of designed systems. This calculation output changes in the final time step of various modeled structures, as illustrated in Fig. 3. As the ion ratio increased, the interaction force between the wall and the fluid decreased, reaching a minimal value of −0.0262 eV/Å. This phenomenon can be explained by examining the behavior of ions within the fluid. At low ion concentrations, the ions were relatively sparse, and the interaction between the fluid molecules and the channel wall was stronger. This stronger interaction forms an ordered 'boundary layer' near the wall, where fluid molecules are more tightly bound, resulting in higher wall-fluid attraction. However, as the ion concentration increased, the ions began to interact more with each other rather than with the wall. This increased ion-ion interaction enhanced ion mobility and reduced the degree of order in the fluid near the wall. Furthermore, at higher ion concentrations, electrostatic repulsion between like-charged ions caused them to 'shield' each other from the wall, further weakening the direct interaction between the fluid and the wall. This shielding effect reduced fluid molecule ordering near the surface, decreasing the wall-fluid interaction force. The enhanced ion mobility allowed the fluid to flow more freely, disrupting the boundary layer and

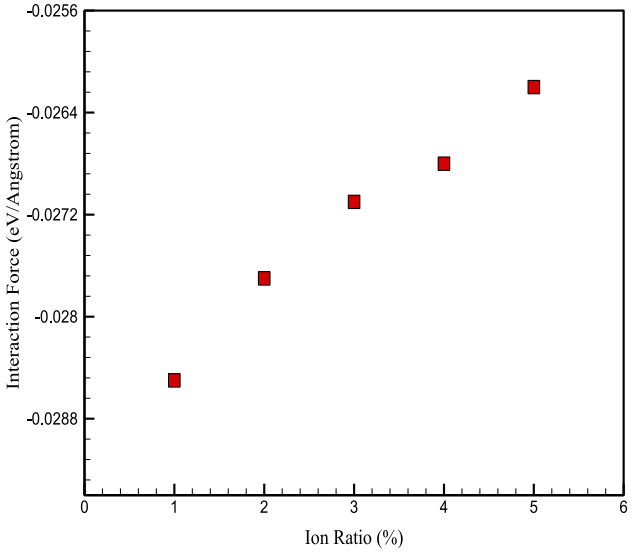

Fig. 3. Changes in the net interaction force between wall atoms and fluid particles in the simulated atomic sample.

decreasing the overall resistance to fluid motion. Consequently, the reduction in wall-fluid interaction force corresponded to an improvement in the physical behavior of ions, as they moved more freely through the fluid. This enhanced mobility of fluid as a whole reflected a system in which ions encountered less resistance from the wall, leading

to better flow properties and increased ion transport efficiency.

The presence of sodium, chlorine, calcium, and magnesium ions played a crucial role in generating electric currents within the studied NF system. In this research, the atomic percentage of these ions was varied at concentrations of 1 %, 2 %, 3 %, 4 %, and 5 %, and the electric current intensity was calculated using MD simulations under controlled conditions (T = 300 K and pressure = 1 bar). The results, shown in Fig. 4, demonstrated a clear trend: as the atomic percentage of ions increased, the electric current intensity also rose. Specifically, as the ionic concentration increased from 1 % to 5 %, the current intensity rose from 5.31 to 5.52 e/ns. This increase in current intensity can be explained by the physical mechanisms involved in ion transport within the system. As the concentration of ions increased, the number of charge carriers available for current conduction also rose. These charge carriers facilitated the flow of electric current through the NF. The higher concentration of ions enhanced ionic mobility, as more ions were available to move through CNTs. Furthermore, as ion concentration increased, the ion transport mechanism improved. Higher ion concentrations strengthened the electrostatic interactions between the ions and surrounding water molecules, aiding in better conduction of electric charge. The increased ion-ion and ion-water interactions enhanced ion transport efficiency, further reducing resistance and contributing to the observed higher current intensity.

Fig. 5 illustrates the relationship between the intensity of NF flow and the ionic percentage of atoms in the simulation box under initial conditions. The results from MD simulations demonstrated that as the ionic percentage increased from 1 % to 5 %, the NF flow intensity rose from 211.31 atoms/ns to 225.43 atoms/ns. This enhancement in flow intensity can be attributed to several interconnected physical phenomena. As the ionic percentage increased, the concentration of ions within the CNT system also rose. This increased ionic concentration enhanced the electroosmotic effect, which occurred due to the interaction of the electric field with mobile ions in the fluid. A higher ionic concentration generated a stronger electric field, exerting a greater driving force on the surrounding water molecules. This force propelled the water molecules through CNTs, directly contributing to the observed increase in NF flow intensity. Furthermore, the elevated ionic concentration reduced ionic resistance within the system. At higher ion levels, the interactions between ions and water molecules became more pronounced. These enhanced ion-water interactions created a coupling effect, where the ions effectively "pull" the water molecules along with them under the influence of an electric field. This coupling facilitated smoother and more efficient water transport through the CNTs. Additionally, the stronger electric field aligned water molecules within the CNTs, minimizing resistance to their flow. This alignment ensured that the movement of water remained more orderly, further contributing to the increase in NF flow intensity. These combined factors, the strengthening of the electroosmotic effect, reduced ionic resistance, and improved ion-water interactions, created a synergistic effect that boosts the overall NF flow.

The results from Fig. 6 show that as the atomic percentage of ions increased from 1 % to 5 %, the maximum density decreased from 4.83 atom/nm^3 to 4.65 atom/nm^3. This decrease in maximum density indicated that the CNT structure became less compact and more porous as ionic concentration rose. Higher ion concentrations disrupted the ordered arrangement of carbon atoms in the CNTs, leading to a less dense and more expanded structure. From a physical standpoint, this change in structure can be explained by the increased mobility of ions. Additionally, the continuous flow of nanofluid inside the CNTs contributed to these changes. As the ionic concentration increased, the number of charge carriers (ions) in the system also rose, enhancing ion movement and fluid flow. This enhanced ion mobility caused the fluid to exert more force on the walls of CNTs, disrupting their closely packed structure and increasing porosity. This structural change can have significant implications for the transport properties and permeability of CNT membranes in applications such as RED. A less compact and more porous structure could increase the membrane's permeability, allowing for better ion

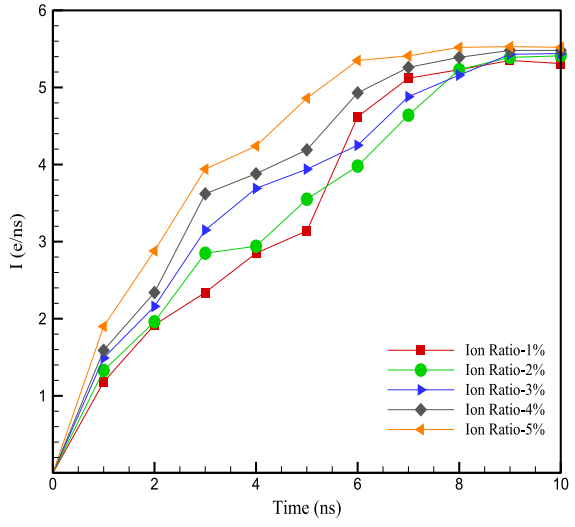

a)

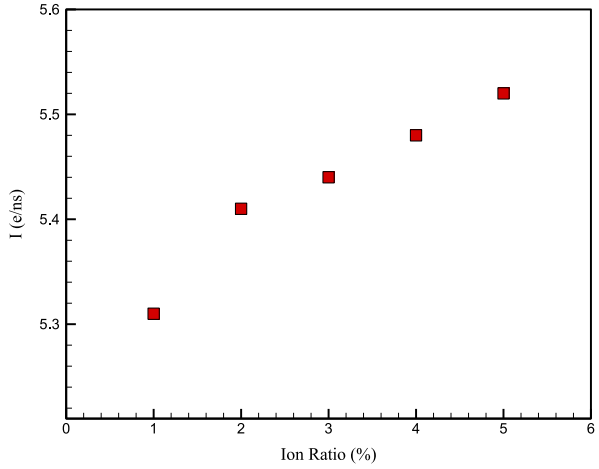

b)

Fig. 4. Variations in electric current intensity in the simulated atomic sample vs. a) simulation time and b)ion ratio.

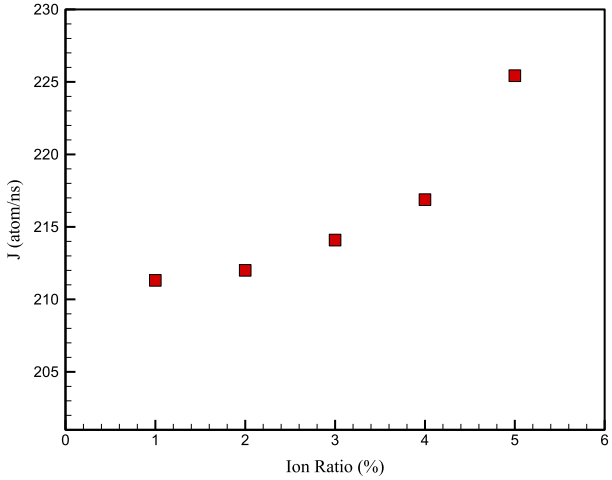

Fig. 5. Variatons in NF flow intensity in the simulated atomic sample.

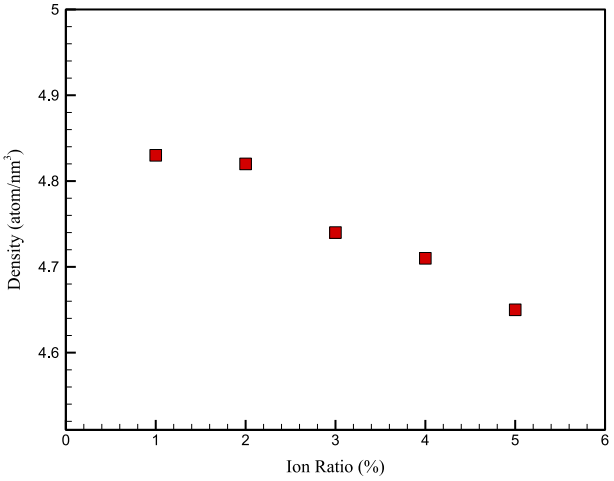

Fig. 6. Variations of the Max atomic density in the simulated atomic sample.

transport. However, this increased permeability may alter the overall efficiency of the system, depending on the specific requirements of the RED process. While greater porosity could facilitate ion flow through the CNTs, it may also reduce control over the ion separation process.

The graph in Fig. 7 illustrates the changes in the number of hydrogen bonds broken as a result of a rise in the percentage of atomic ions at initial conditions of T = 300 K and pressure = 1 bar. The final NF was more strongly displaced, as mentioned in the preceding section, due to the rise in atomic ions. The number of broken hydrogen bonds increased due to high mobility and the creation of a continuous flow of NF inside the carbon channel, increasing the intensity within the channel. Consequently, the structural transformation behavior in the samples was observed more intensely. From a numerical perspective, the number of broken hydrogen bonds increased from 116 to 133 with the increase in the ionic proportion of atoms from 1 % to 5 %. This rise indicated that a greater proportion of ions had a substantial effect on the hydrogen bonding structure among water molecules within the CNTs. The disturbance of the hydrogen bond network may affect the overall movement and dynamics of water transport within the system. Technically, the structural outputs from the modeled samples were used for this computation. By helping this structural output, VMD software can compute the temporal evolution, including the breakdown of atomic bonds as a consequence of their separation. This method explained how

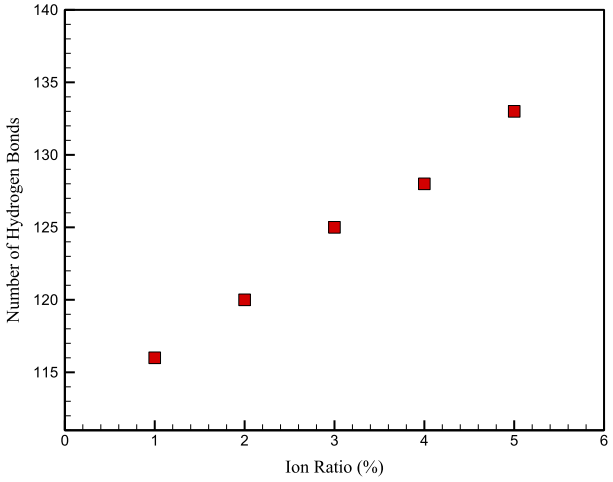

Fig. 7. Variations in the number of broken hydrogen bonds in the simulated atomic sample.

the mean atomic distance varied across samples, affecting the performance of each sample in the present study. It indicated structural changes that can impact permeability, ionic transport, and particle diffusion through the membrane. This disruption of the hydrogen bond network altered pore structure and connectivity, potentially affecting the efficiency and stability of the RED process. Nevertheless, it should be noted that in the simulated atomic structures, the samples maintained thermodynamic stability despite the mentioned time evolution and showed appropriate atomic behavior. The numerical results of this part are reported in Table 2.

The numerical values of NF electric current intensity, NF current intensity, Max density and the number of bonds created in terms of the percentage of atomic ions at a T = 300 K and a pressure = 1 bar are shown in Table 2.

5. Conclusion

This study employed MD simulations to explore the transport of water through CNTs under the effect of an electric current. The main objective was to assess how varying ion atomic ratios affect several key parameters that govern the system's behavior. These parameters include electric current intensity, NF current intensity, maximum density, the number of hydrogen bonds, and interaction energy as ion concentration changes. The study specifically aimed to investigate how these changes influence ion mobility, water permeability, and interactions between the ions and the CNT structure. The research was conducted in two phases: first, equilibration, followed by the examination of atomic transformation processes and the creation of different atomic ratios in the samples. The results from the first phase are as follows:

- The kinetic energy in the atomic sample converged to a numerical value of 0.162 eV after 10 ns.
- The potential energy in the atomic samples converged to 2.048 after 10 ns.

These convergences indicated the limitations on structural mobility over the simulation time. They also suggested the presence of an average attractive force among the atoms in different parts of the simulation box. After observing equilibrium in the simulated atomic sample, we achieved atomic transformation and created various atomic ratios in the defined samples.

- Increasing the ion ratios in the NF resulted in an increase in electric current intensity from 5.31 to 5.52 e/ns.
- The higher ion concentration in the NF system led to a greater density of charge carriers, which enhanced ionic mobility and improved the ion transport mechanism through the CNTs.
- The intensity of NF flow increased numerically as the ionic percentage of atoms rose from 1 % to 5 %, rising from 211.31 to 225.43 atoms/ns.
- This increase in NF flow intensity was attributed to a reduction in ionic resistance and enhanced ion-water interactions, which facilitated nanofiltration.

Table 2
Variations in the intensity of the electric current of the NF, the Max density, and the number of bonds created in terms of the percentage of atomic ions.

The atomic percentage of defined ions	Interaction Force (eV/Angstrom)	Electric current intensity (e/ns)	Max density (atoms/nm^3)	NF flow intensity (atom/ns)	Number of hydrogen bonds
1	−0.0285	5.31	4.83	211.31	116
2	−0.0277	5.41	4.82	212.00	120
3	−0.0271	5.44	4.74	214.09	125
4	−0.0268	5.48	4.71	216.88	128
5	−0.0262	5.52	4.65	225.43	133

- As the atomic percentage of defined ions increased from 1 % to 5 %, the maximum density in the structure decreased from 4.83 to 4.65 atoms/nm^3.
- The reduced Max density suggested that higher ionic concentration promoted increased mobility and a more stable flow inside the NTs channel.
- The number of broken hydrogen bonds increased from 116 to 133 with the rise in atomic ion concentration to 5 %.
- This increase in broken hydrogen bonds indicated that the ionic concentration significantly disrupted the hydrogen bonding network of water molecules within the CNTs.
- The disruption of hydrogen bonding network could potentially affect the total water transport and flow dynamics within the system.

6. Future research

Based on the research details provided, some key areas that could be studied in future research include:

- Exploring the Optimal Ion Ratio:
- Investigating the Underlying Mechanisms:
- Scaling and Optimization Studies:
- Coupling with Other Processes:

Further examine the precise processes affecting the changes in hydrogen bond interactions, NF flow, and electric current as a function of ion ratio. Examine how surface charge effects, ion hydration, and ion-water interactions influence the observed behaviors. Analyze the performance of the CNT system at various scales by adjusting the CNTs' length, diameter, or quantity. To enhance water transport and energy efficiency further, optimize system design parameters, including material properties and CNT geometry. Additionally, investigate how the CNT system may be integrated with other methods of energy conversion or water treatment, such as catalytic reactions, electrochemical energy storage, or reverse osmosis. By addressing these prospective research directions, scientists and engineers can deepen their understanding of water transport in CNT systems under electric fields. This will lead to advancements in water purification, energy storage, and other related applications.

CRediT authorship contribution statement

Ali B.M. Ali: Formal analysis, Data curation, Conceptualization. **Karwan Hussein Qader:** Validation, Methodology. **Murtadha M. Al-Zahiwat:** Investigation, Writing – original draft. **Narinderjit Singh Sawaran Singh:** Formal analysis, Data curation, Conceptualization. **Soheil Salahshour:** Investigation, Writing – original draft. **S. Mohammad Sajadi:** Formal analysis, Data curation, Conceptualization. **Ali Mokhtarian:** Formal analysis, Data curation, Conceptualization.

Declaration of competing interest

The authors declare that they have no known competing financial interests or personal relationships that could have appeared to influence the work reported in this paper.

Appendix

A. Simulation Method

MD simulation focuses on understanding the factors that drive particle movement. In this context, each small particle is always considered to be connected to its surroundings and influenced by them. Thus, the movement of a specific particle is influenced by the presence and arrangement of neighboring particles [28]. The study of MD simulation involved examining how particles interacted with one another based on the principles of physics over a period [29].

MD simulation uses a potential function or specific parameters to describe how the system components interact. In molecular modeling, the force field is a set of formulas and numbers used to calculate the energy associated with a system of particles in an MD simulation. The total energy of a system is calculated by summing the bonding forces with the non-cohesive forces [28].

$$E_{total} = E_{bonded} + E_{nonbonded} \tag{a-1}$$

The absence of a connection among the particles resulted in various types of potential energy within non-bonded interactions. This energy arises from a combination of Lennard-Jones, Tersoff, and Coulomb potential functions. Lennard-Jones potential function is a simple equation that predicts the interaction between two uncharged particles or molecules [30–32]. The most common relation of the Lennard-Jones potential function is in the form of Eq. (a-2).

$$U_{LJ} = 4\varepsilon\left[\left(\frac{\sigma}{r}\right)^{12} - \left(\frac{\sigma}{r}\right)^{6}\right] \tag{a-2}$$

ε_{ij} represents the well's depth, σ_{ij} shows the boundary where the potential became zero, and r_{ij} is the distance among the particles in Eq. (a-2). The values of σ and ε for each particle in the simulation can be found in Table a-1.

Table a-1
Parameters of Lennard-Jones potential function for particles in MD simulations [33,34].

Particle type	σ (Å)	ε (kcal/mol)
H	0.000	0.000
O	3.166	0.1553
C	3.851	0.105
Na	2.983	0.030
Cl	3.947	0.227
Si	4.295	0.402
Ca	3.399	0.238
Mg	3.021	0.111

The coefficients σ_{ij} and ε_{ij} are defined by helping the following equations [33]:

$$\varepsilon_{ij} = \sqrt{\varepsilon_i \varepsilon_j} \tag{a-3}$$

$$\sigma_{ij} = \frac{\sigma_i + \sigma_j}{2} \tag{a-4}$$

The electric or electrostatic potential energy comes from the forces caused by Coulomb's constant. The energy is associated with configuring a collection of charges within a specific arrangement. This explains how some particles in a system can either repel or attract toward each other because of their static electric charges [32]. Electric potential energy is defined by Eq. (a-5).

$$U_{ij}(r) = \frac{-1}{4\pi\varepsilon_0} \frac{q_i q_j}{{r_{ij}}^2} \tag{a-5}$$

In Eq. (a-5), qj and qi are the electric charges of particles i and j, rij is the distance among the charges, and ε0 indicates the electrical permeability of free space, numerically equal to 8.85×10^{-12} F m^{-1}. An ensemble in the simulated system allows us to evaluate the correlation between simulated outcomes and experimental data. Ensembles provide essential information about T, pressure, energy, and the arrangement of a system in equilibrium. Ensembles are typically classified into different types [28]. Canonical and micro-canonical ensemble groups were used in the simulations carried out in this research.

Data availability

No data was used for the research described in the article.

References

[1] R. Messmer, P. Stamp, Trends in drought research, Agricul. Natural Re. 44 (4) (2010) 507–516.
[2] H. Ahani, et al., An investigation of trends in precipitation volume for the last three decades in different regions of Fars province, Iran, Theor. Appl. Climatol. 109 (3) (2012) 361–382.
[3] M. Shojaei-Miandoragh, M. Bijani, E. Abbasi, Farmers' resilience behaviour in the face of water scarcity in the eastern part of Lake Urmia, Iran: an environmental psychological analysis, Water Environ. J. 34 (4) (2020) 611–622.
[4] M. Bradbury, Water City: Practical Strategies for Climate Change, Routledge, 2020.
[5] Y. Osada, T. Nakagawa, Membrane Science and Technology, CRC Press, 1992.
[6] P.T. Lynch, M.R. Davey, Electrical Manipulation of Cells, Springer Science & Business Media, 2012.
[7] J. Veerman, M. Saakes, S.J. Metz, G. Harmsen, Reverse electrodialysis: evaluation of suitable electrode systems, J. Appl. Electrochem. 40 (2010) 1461–1474.
[8] W. Choi, Z.W. Ulissi, S.F. Shimizu, D.O. Bellisario, M.D. Ellison, M.S. J.N.c. Strano, Diameter-dependent ion transport through the interior of isolated single-walled carbon nanotubes 4 (1) (2013) 2397.
[9] H. Zhang, et al., Combined effects of surface charge and pore size on co-enhanced permeability and ion selectivity through RGO-OCNT nanofiltration membranes 52 (8) (2018) 4827–4834.
[10] A. Cipollina, et al., Reverse electrodialysis: applications, in: Sustainable Energy from Salinity Gradients, Elsevier, 2016, pp. 135–180.
[11] E. Ganesh, Single walled and multi walled carbon nanotube structure, synthesis and applications, Int. J. Innovative Technol. Explor. Eng. 2 (4) (2013) 311–320.
[12] K. Szendi, C. Varga, Lack of genotoxicity of carbon nanotubes in a pilot study, Anticancer Res. 28 (1A) (2008) 349–352.
[13] W. Andreoni, The Physics of Fullerene-Based and Fullerene-Related Materials, Springer Science & Business Media, 2000.
[14] V.N. Popov, Carbon nanotubes: properties and application, Mater. Sci. Eng. R Rep. 43 (3) (2004) 61–102.
[15] H. Fattahi, M. Koselou, Y.M. Oskoei, Selective separation and removal of toxic heavy metal ions from water by magnetic ion-imprinted nano polymers, Polymer (Korea) 6 (4) (2017) 20–35.
[16] A. Lohrasebi, S. Rikhtehgaran, Ion separation and water purification by applying external electric field on porous graphene membrane, Nano Res. 11 (4) (2018) 2229–2236.
[17] A. Khataee, J. Azamat, G. Bayat, Separation of nitrate ion from water using silicon carbide nanotubes as a membrane: insights from molecular dynamics simulation, Comput. Mater. Sci. 119 (2016) 74–81.
[18] N.H. Othman, N. Kabay, E. Guler, Principles of reverse electrodialysis and development of integrated-based system for power generation and water treatment: a review, Rev. Chem. Eng. (2021) 235716351, https://doi.org/10.1515/revce-2020-0070.
[19] J.G. Hong, B. Zhang, S. Glabman, N. Uzal, X. Dou, H. Zhang, X. Wei, Y. Chen, Potential ion exchange membranes and system performance in reverse electrodialysis for power generation: a review, J. Membr. Sci. 486 (2015) 71–88.
[20] W. Li, W.B. Krantz, E.R. Cornelissen, J.W. Post, A.R. Verliefde, C.Y. Tang, A novel hybrid process of reverse electrodialysis and reverse osmosis for low energy seawater desalination and brine management, Appl. Energy 104 (2013) 592–602.
[21] N.Y. Yip, M. Elimelech, Comparison of energy efficiency and power density in pressure retarded osmosis and reverse electrodialysis, Environ. Sci. Technol. 48 (18) (2014) 11002–11012.
[22] A. Panahi, P. Sadeghi, A. Akhlaghi, M.H.J.D. Sabour, R. Materials, Investigating the Effect of Single-Walled Carbon Nanotubes Chirality on the Electrokinetics Transport of Water and Ions: A Molecular Dynamics Study, vol. 110, 2020 108105.
[23] J. Shi, X. Zhou, P. Jia, K. Cai, Ion separation together with water purification via a new type of nanotube: a molecular dynamics study, Int. J. Mol. Sci. 24 (7) (2023) 6677.
[24] N. Naghdian, Z. Ahadi, J. Davoodi, C.F. Matta, M. Shadman, Electrodialysis desalination: borophene membrane for ion separation using non-equilibrium molecular dynamics, J. Mol. Liq. 396 (2024) 123945.
[25] A. Hasanzadeh, M. Alizadeh, N. Ajalli, J. Azamat, M. Jahanshahi, Molecular dynamic simulation and artificial neural network (ANN) modeling of the functionalized graphene oxide membranes on Cr (VI) ion removal through electrodialysis method, J. Mol. Liq. 383 (2023) 122083.
[26] Y. Li, A.B. Ali, N.E.F. Tapia, N. Kamolova, S. Salahshour, R. Sabetvand, Effect of channel roughness on the particle diffusion and permeability of carbon nanotubes in reverse electrodialysis process applying molecular dynamics simulation, J. Mol. Graph. Model. (2024) 108899.
[27] D.J. Jasim, A.B. Ali, A.A. Almehizia, A.A. Zen, S. Salahshour, S. Esmaeili, Effect of external force on the dispersion of particles and permeability of substances via carbon nanotubes in reverse electrodialysis using molecular dynamics simulation, Intern. J. Thermofluids 24 (2024) 100915.
[28] D.C. Rapaport, The Art of Molecular Dynamics Simulation, Cambridge university press, 2004.
[29] B.J. Alder, T.E. Wainwright, Studies in molecular dynamics. I. General method, J. Chem. Phys. 31 (2) (1959) 459–466.
[30] J.E. Lennard-Jones, Cohesion, Proc. Phys. Soc. 43 (5) (1931) 461.
[31] M.S. Daw, M.I. Baskes, Embedded-atom method: derivation and application to impurities, surfaces, and other defects in metals, Phys. Rev. B 29 (12) (1984) 6443.
[32] P.G. Huray, Maxwell's Equations, John Wiley & Sons, 2011.
[33] H.J. Berendsen, J.R. Grigera, T.P. Straatsma, The missing term in effective pair potentials, J. Phys. Chem. 91 (24) (1987) 6269–6271.
[34] A.K. Rappé, C.J. Casewit, K. Colwell, W.A. Goddard III, W.M. Skiff, UFF, a full periodic table force field for molecular mechanics and molecular dynamics simulations, J. Am. Chem. Soc. 114 (25) (1992) 10024–10035.